④

REPORT SD-TR-89-40

AD-A211 141

Master Oscillator with Power Amplifiers: Performance of a Two–Element CW HF Phased–Laser Array

J. M. BERNARD, R. A. CHODZKO, and J. G. COFFER
Aerophysics Laboratory
The Aerospace Corporation
El Segundo, CA 90245

15 June 1989

Prepared for

WEAPONS LABORATORY
Kirtland Air Force Base
Albuquerque, NM 87115

SPACE SYSTEMS DIVISION
AIR FORCE SYSTEMS COMMAND
Los Angeles Air Force Base
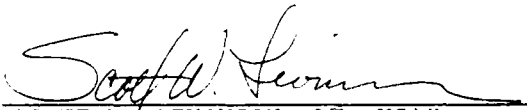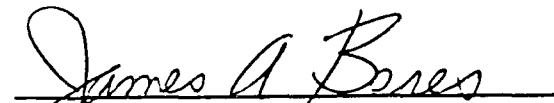P.O. Box 92960
Los Angeles, CA 90009-2960

DTIC
ELECTE
AUG 1 1 1989
S
B
D

This report was submitted by The Aerospace Corporation, El Segundo, CA 90245, under Contract No. F04701-85-C-0086-P00019 with the Space Systems Division, P.O. Box 92960, Los Angeles, CA 90009-2960. It was reviewed and approved for The Aerospace Corporation by W. P. Thompson, Director, Aerophysics Laboratory. Lt Scott W. Levinson was the Air Force project officer.

This report has been reviewed by the Public Affairs Office (PAS) and is releasable to the National Technical Information Service (NTIS). At NTIS, it will be available to the general public, including foreign nationals.

This technical report has been reviewed and is approved for publication. Publication of this report does not constitute Air Force approval of the report's findings or conclusions. It is published only for the exchange and stimulation of ideas.

SCOTT W. LEVINSON, LT, USAF
MOIE Project Officer
AFSTC/WCO OL-AB

JAMES A. BERES, LT COL, USAF
Director, AFSTC/WCO OL-AB

REPORT DOCUMENTATION PAGE

1a. REPORT SECURITY CLASSIFICATION	1b. RESTRICTIVE MARKINGS
Unclassified	

2a. SECURITY CLASSIFICATION AUTHORITY	3. DISTRIBUTION/AVAILABILITY OF REPORT
2b. DECLASSIFICATION/DOWNGRADING SCHEDULE	Approved for public release; distribution unlimited.

4. PERFORMING ORGANIZATION REPORT NUMBER(S)	5. MONITORING ORGANIZATION REPORT NUMBER(S)
TR-0088(3060)-1	SD-TR-89-40

6a. NAME OF PERFORMING ORGANIZATION	6b. OFFICE SYMBOL (If applicable)	7a. NAME OF MONITORING ORGANIZATION
The Aerospace Corporation Laboratory Operations		Space Systems Division

6c. ADDRESS (City, State, and ZIP Code)	7b. ADDRESS (City, State, and ZIP Code)
El Segundo, CA 90245-4691	Los Angeles Air Force Base Los Angeles, CA 90009-2960

8a. NAME OF FUNDING/SPONSORING ORGANIZATION	8b. OFFICE SYMBOL (If applicable)	9. PROCUREMENT INSTRUMENT IDENTIFICATION NUMBER
		F04701-85-C-0086-P00019

8c. ADDRESS (City, State, and ZIP Code)	10. SOURCE OF FUNDING NUMBERS			
	PROGRAM ELEMENT NO.	PROJECT NO.	TASK NO.	WORK UNIT ACCESSION NO.

11. TITLE (Include Security Classification)

Master Oscillator with Power Amplifiers: Performance of a Two-Element CW HF Phased-Laser Array

12. PERSONAL AUTHOR(S)
Bernard, Jay M.; Chodzko, Richard A.; and Coffer, John G.

13a. TYPE OF REPORT	13b. TIME COVERED	14. DATE OF REPORT (Year, Month, Day)	15. PAGE COUNT
	FROM _____ TO _____	1989 June 15	23

16. SUPPLEMENTARY NOTATION

17. COSATI CODES			18. SUBJECT TERMS (Continue on reverse if necessary and identify by block number)
FIELD	GROUP	SUB-GROUP	
			HF Laser Oscillator/Amplifier
			Laser Phased Laser Array

19. ABSTRACT (Continue on reverse if necessary and identify by block number)

The experimental performance of a two-element phased array of multiline continuous-wave hydrogen-fluoride chemical lasers in the master oscillator with power amplifiers (MOPA) configuration has been measured. The mutual coherence of the two amplified beams was inferred from measurements of the visibility of interference fringes obtained when the beams were overlapped in the near field. When the optical path difference for the two beams was minimized, multiline visibilities of 0.90 ± 0.02 were measured. White-light interferometry was used to equalize the optical path lengths. Spectral mismatch between the master oscillator output and the amplifier's preferred gain distribution affected neither the amplification factor nor the mutual coherence of the amplified beams. The effect of spatial coherence of the master oscillator beam on these near-field measurements, and the eventual requirement of far-field measurements to precisely optimize path lengths, is discussed. Spectral data, amplification factors, and mutual coherence measurements are shown, and the resulting phased-array far-field performance is presented.

20. DISTRIBUTION/AVAILABILITY OF ABSTRACT	21. ABSTRACT SECURITY CLASSIFICATION
[X] UNCLASSIFIED/UNLIMITED ☐ SAME AS RPT. ☐ DTIC USERS	Unclassified

22a. NAME OF RESPONSIBLE INDIVIDUAL	22b. TELEPHONE (Include Area Code)	22c. OFFICE SYMBOL

DD FORM 1473, 84 MAR   83 APR edition may be used until exhausted.   SECURITY CLASSIFICATION OF THIS PAGE
All other editions are obsolete

PREFACE

1

CONTENTS

FIGURES

I. INTRODUCTION

Master oscillator with power amplifier (MOPA) configurations have been proposed[1-4] for phased arrays of laser light sources. The master oscillator of a MOPA is a laser whose output is split into several beams, each of which is amplified by single or multiple passes through separate gain regions. The outputs of the many amplifiers are expected to preserve the phase distribution of the master-oscillator beam, and thus should be mutually coherent with each other. The critical issues concerning multiline MOPA systems include:

- Is the phase distribution of the master oscillator preserved upon amplification?

- What is the performance penalty paid for a spectral mismatch between the master oscillator output and the amplifier gain distribution?

- Can near-field phase measurements ensure optimum far-field performance?

Early experiments[3,4] using beamsplitter sampling on continuous-wave (CW) hydrogen-fluoride (HF) chemical lasers demonstrated that complete phase matching of an amplified multiline beam with an unamplified sample of the same beam was feasible. This report describes results of experiments using the MOPA configuration as a two-element phased array of multiline CW HF lasers in order to investigate the issues mentioned above. We quantify the mutual coherence of the beams emerging from the two apertures via measurements of the visibility of the interference fringes obtained by overlapping the two beams in the near field. Typical amplification factors for the two beams are presented, and the effect of spectral mismatch is presented. We discuss a comparison of the mutual coherence of beams obtained by wavefront division of the master oscillator beam (using a mirror edge) vs the amplitude division technique (using a transmissive/reflective beamsplitter). The relation between these near-field measurements and the ultimate requirement for far-field diagnostics is presented, and is verified by our measurements of far-field phased array performance.

7

II. EXPERIMENTAL APPARATUS

Figure 1 is a schematic diagram of our MOPA/phased array optical system using a partial-aperture beamsplitting configuration. The beam from a multiline, CW HF subsonic "probe" laser[5] is expanded to 1 cm diameter and propagated (in a single pass) through an arc-driven supersonic CW HF gain medium.[6] The amplified beam is split into two by the externally coated faces of the beamsplitting prism. Note that this is the wavefront-division type of beamsplitter. The beam reflected upward traverses a system of fixed mirrors to the phased-array output aperture, which is another externally coated prism. The optical train traversed by the amplified beam that is reflected downward by the beamsplitting prism includes an "optical trombone"--two mirrors attached to a translation stage to provide a variable optical path length for that beam without affecting its alignment. This provides a means to accomplish the necessary equalization of the optical path lengths required for multiline phase matching.[3,4]

The diagnostic arrangement for the MOPA experiments is shown schematically in Fig. 2. The individual beams can be routed to power meters by inserting a third externally coated prism into the diagnostic path, using a removable kinematic mount. These power meters are used to measure the amplification factor for the individual beams, and to ensure proper positioning of the two beams within the gain region. With the third prism removed, the beams can be directed to an Optics Engineering HF laser spectrum analyser for measurement of their spectral content, by use of another kinematic mount. Otherwise, the beams proceed to the rotating-mirror beam scanning diagnostic. This arrangement of rotating mirror, pinhole, and detector provides a one-dimensional scan of the intensity distribution at the plane of the pinhole. When the mirror M_1 is flat, this diagnostic records a scan of the near-field fringes obtained when the two beams are overlapped. When M_1 is replaced by a concave mirror of the appropriate focal length, the rotating mirror apparatus displays the centerline scan of the far-field focal spot of the two beams. Single-line

intensity distributions are obtained by inserting an appropriate filter in front of the pinhole. These data are collected by a Norland model 3001 digital oscilloscope and recorded on magnetic disk.
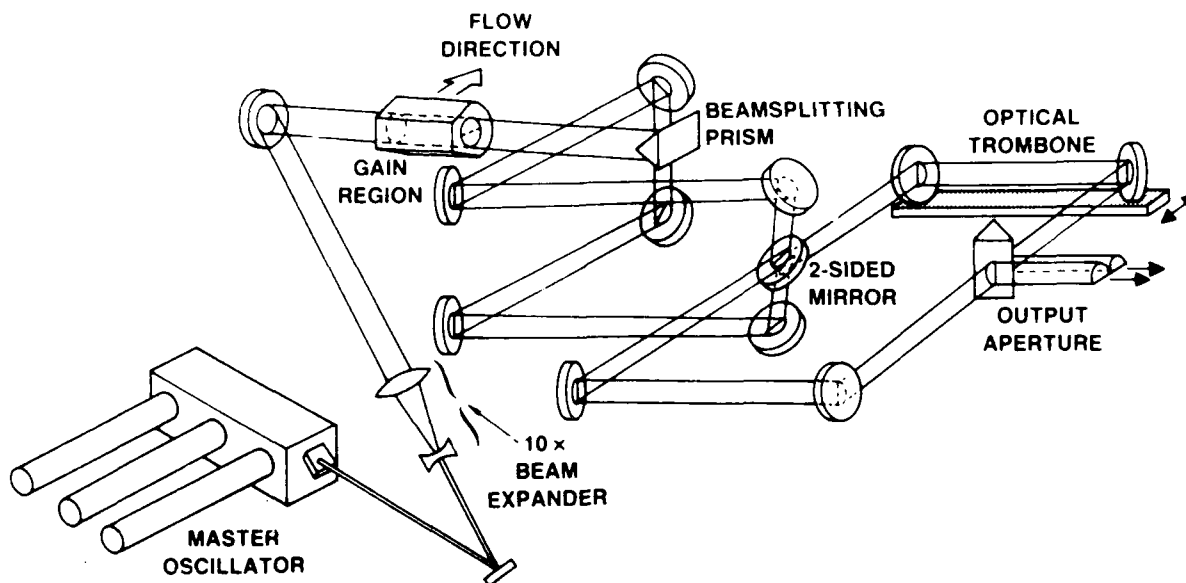

Fig. 1.   Schematic Diagram of the Master Oscillator with Power
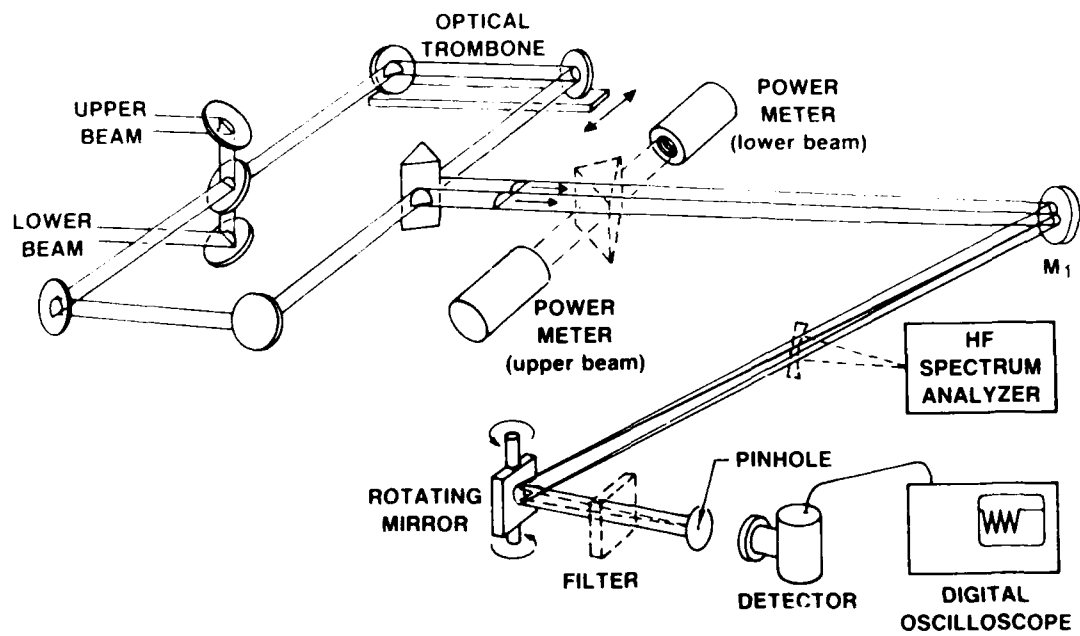   Amplifier Experimental Configuration

Fig. 2.   Schematic Diagram of the Phased-Array Diagnostic System

III. OPTICAL PATH EQUALIZATION

Whereas two single-line beams can be made to constructively interfere when their path lengths are different integral numbers of wavelengths, the multiline nature of the HF laser requires that the optical path lengths for the two beams from the beamsplitting prism to the diagnostic location be exactly equal.[3,4] Only at this zero optical path difference (zero OPD) condition will all of the spectral lines constructively interfere at the same location. Zero OPD can be found by translating the optical trombone until the interference fringes from the split master-oscillator beam display a maximum visibility. Unless the maximum visibility is very close to 1, however, a secondary maximum in visibility (several wavelengths away from zero OPD) could be mistaken for the zero OPD location. Furthermore, if only a few lines are output by the master oscillator, many secondary maxima exist, and their visibilities are very close to the maximum value. For these reasons, we used an independent measure of the zero OPD condition: white-light interferometry. White light interference fringes can only be observed when the path lengths of the interfering beams are within a few wavelengths of being equal.[3] Also, their visibility has a single, distinct maximum at zero OPD. These considerations are illustrated by Fig. 3 (taken from Ref. 3), which is an experimental measurement of the fringe intensity in the output of a Mach-Zehnder interferometer as a function of OPD for both a multiline HF laser beam and a zirconium-arc white-light source.

In our experiment, we used a three-legged version of a Michelson interferometer to equalize the path lengths of the two test legs with that of a third reference leg. Shown schematically in Fig. 4, a beam of white light from a tungsten bulb is split by a full-aperture (amplitude division) beamsplitting plate. The reflected beam becomes the reference leg, which includes a compensating plate of the same thickness as the beamsplitting plate, and the transmitted beam is split into two half-apertures by a beamsplitting prism (wavefront division). After aligning all of the legs

13

a. HF LASER

NEAR-FIELD
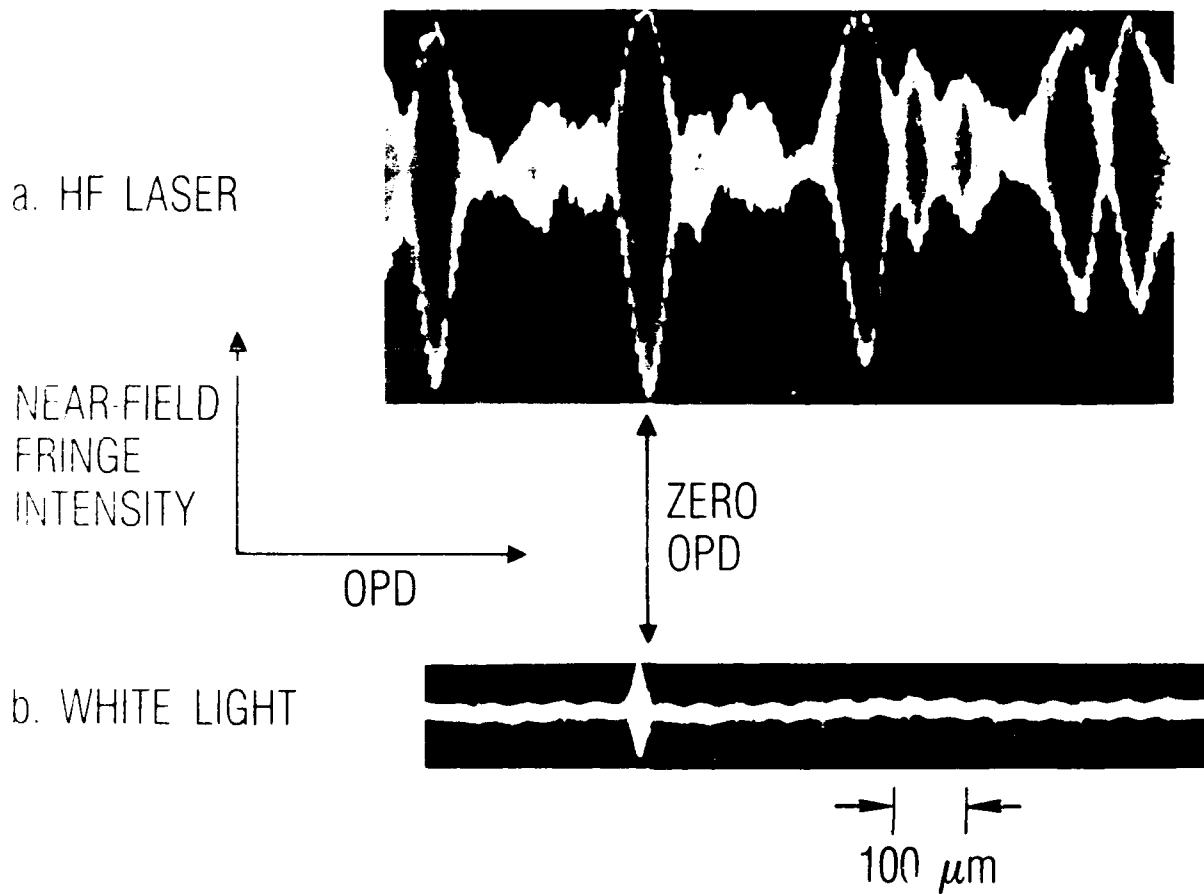FRINGE
INTENSITY

OPD

ZERO
OPD

b. WHITE LIGHT

100 μm

Fig. 3. Fringe Intensity as a Function of OPD for a Mach-Zehnder
Interferometer Illuminated by (a) Multiline HF Laser,
and (b) a White Light Source

REFERENCE
LEG

TROMBONE
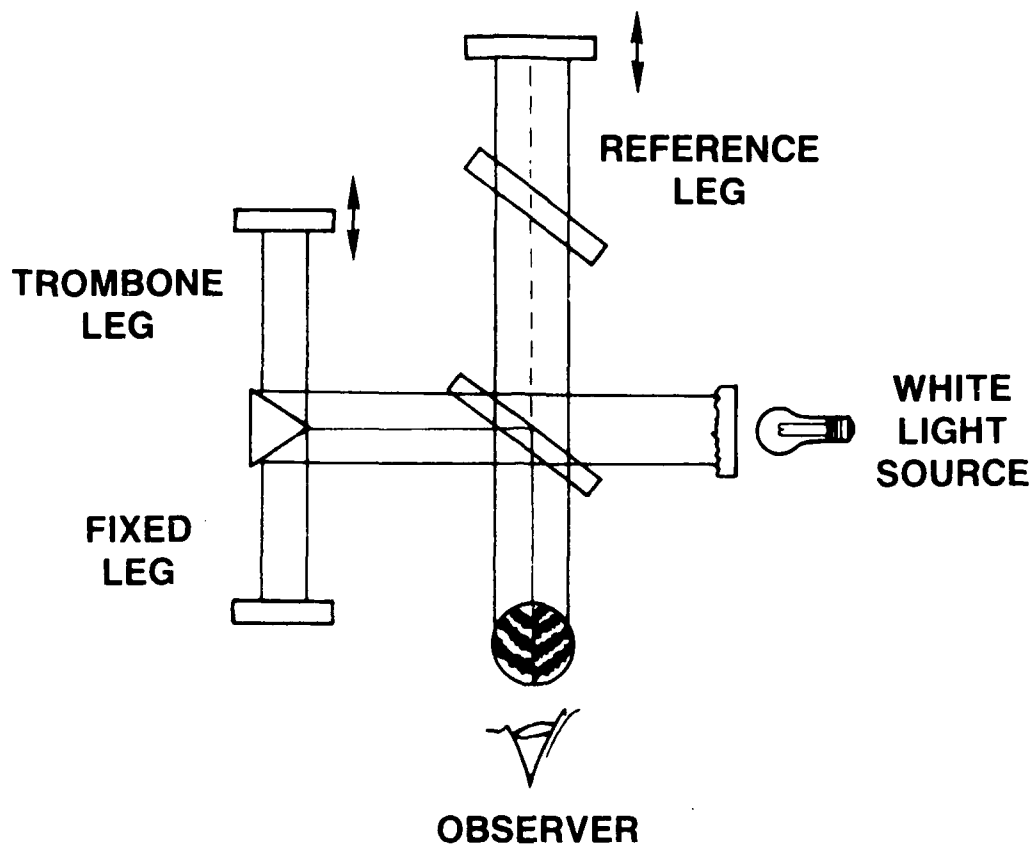LEG

WHITE
LIGHT
SOURCE

FIXED
LEG

OBSERVER

Fig. 4. Schematic Diagram of a Three-Legged White-Light
Michelson Interferometer

of the interferometer for tilt (using a visible alignment laser), the
length of the reference leg is adjusted until white light fringes are
observed in the right-hand output aperture. The optical trombone is then
adjusted until fringes are observed in the left-hand aperture. When the
interferometer is thus aligned, the central fringe (the one with maximum
visibility) is seen in both apertures, and the lengths of all three
interferometer legs are equal within 0.2 micron. Using photodetectors,
precise position encoders, and fringe-counting electronics, zero-OPD could
be diagnosed within 0.05 micron. Figure 5 is a drawing of the actual
layout of the three-legged interferometer used to equalize the optical
paths in our MOPA. It was aligned by the same procedure discussed above,
but note that the retroreflector for both test legs is the same flat
mirror. This ensures equal optical paths for the split master oscillator
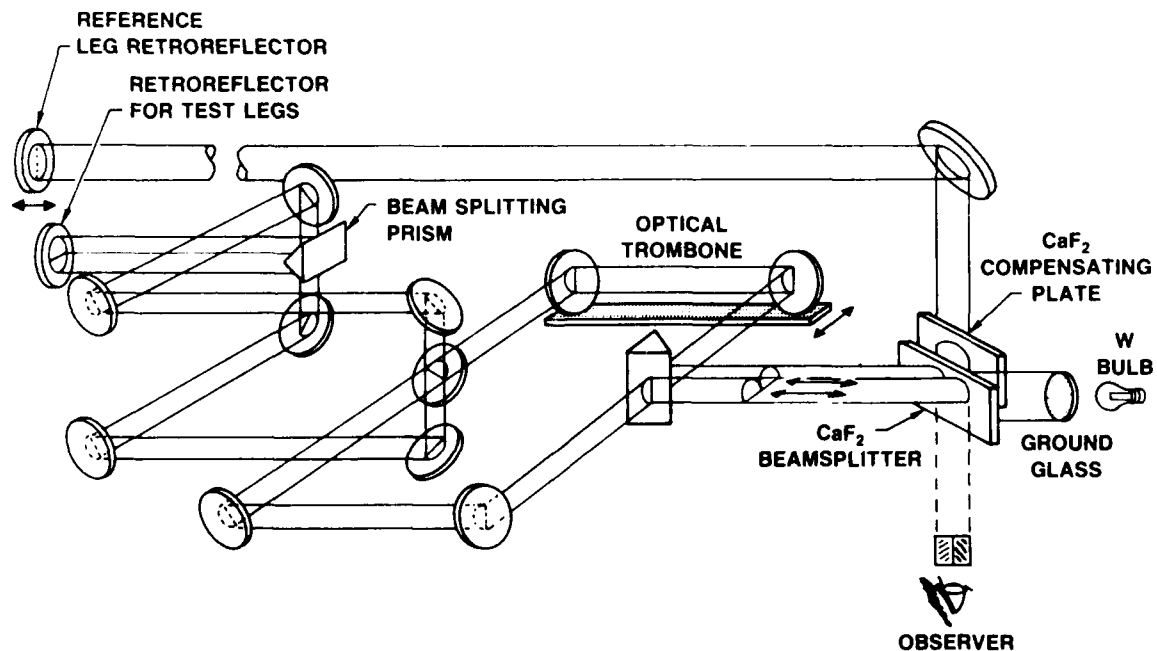beams from the beamsplitting prism to the output aperture.

Fig. 5. Drawing of the Michelson Interferometer Setup
as it was Used on Our Optical System

The average power in the split master-oscillator beams was typically 3 watts each (at the diagnostic location). Upon amplification, beams of 6 watts each were obtained for either of two different master oscillator output spectra. Figure 6 is a typical thermal image of the focal plane of the HF laser spectrum analyzer under conditions of the best spectral match between oscillator and amplifier (best spectral match is determined as the spectrum that is typically output from the arc-driven amplifier when it is operated as an oscillator). It shows that the dominant lines are $P_1(6)$, $P_2(5)$, and $P_2(6)$, with contributions from $P_1(7)$ and $P_2(7)$. When the master oscillator output was adjusted so that $P_2(8)$ was the dominant line, the amplification factor was still 2, owing to the rapid cross-relaxation of the vibration-rotation levels of the HF medium. The mutual coherence measurements quoted below did not change when the oscillator spectrum was changed.

Typical oscilloscope traces of the multiline near-field interference fringes are shown in Fig. 7. These traces were obtained at the zero OPD setting of the optical trombone. Figure 7a shows fringes from the split master oscillator beam without amplification, while Fig. 7b is of the MOPA output (with amplification). In either case, the measured visibility
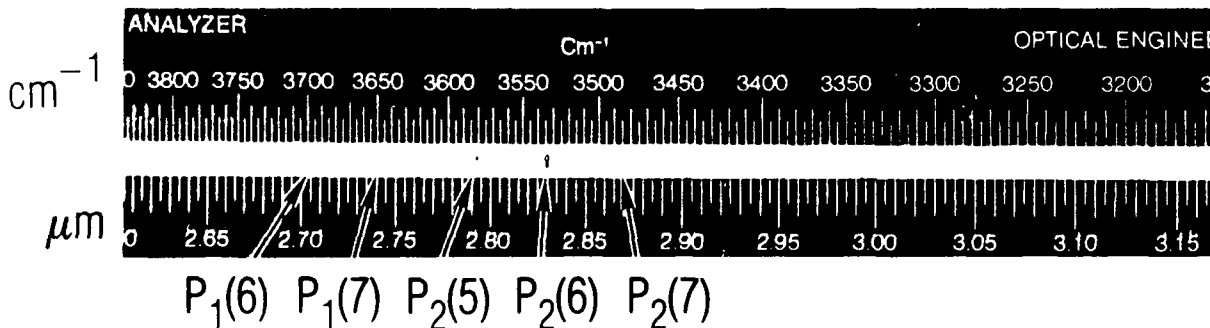

Fig. 6.   Thermal Image of the Focal Plane of the HF Laser Spectrum Analyzer, with the Spectral Lines Identified

(after correction for the size of the pinhole with respect to the fringe spacing) of the maximum-visibility fringe is 0.90 ± 0.02. The degradation from a visibility of 1 is a property of the master oscillator beam and the diagnostic arrangement; it is important to note that there is no measurable degradation in visibility due to amplification of the master oscillator beam. Figure 8 is an oscilloscope trace of the $P_2(6)$ single-line component of the near-field fringe pattern, for which the measured visibility is 0.98, with or without amplification. We therefore conclude that amplification does preserve the phase coherence of the master oscillator beam, and the MOPA is therefore a viable concept for obtaining phased arrays of multiline HF lasers.
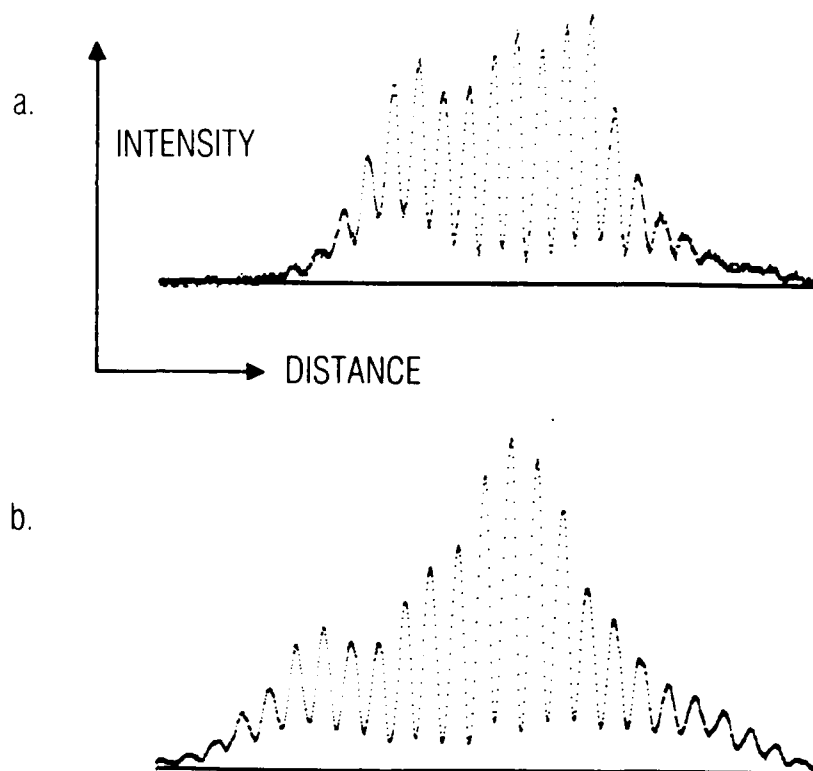
a.

INTENSITY

DISTANCE

b.

Fig. 7. Horizontal Scan of the Near-Field Multiline
Interference Fringes (a) for the Master
Oscillator Beams Without Amplification, and
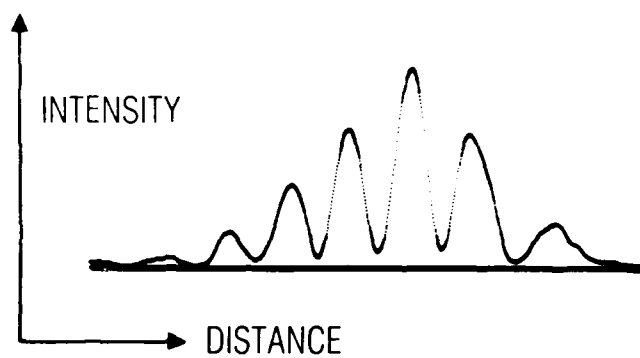(b) for the Amplified MOPA Output Beams

Fig. 8. Horizontal Scan of the $P_2(6)$ Component
of the Near-Field Interference Fringes
with Amplification

V. FAR-FIELD MEASUREMENTS

The performance of a phased-array optical system is ultimately measured as the far-field brightness. Crucial to obtaining the maximum brightness is path-length equalization for each of the phased-array output apertures, which in turn depends on the ability to diagnose path length differences. Maximizing the visibility of near-field fringes is one approach to obtaining zero OPD, but the measured visibility is greatly affected by the sampling technique used to obtain the interfering beams. Near-field fringe visibility using wavefront division is a function of the spatial mutual coherence of the two beams, while the far-field measurement is the overlapping of essentially plane waves. Furthermore, the far-field brightness is a more sensitive function of path length differences than is near-field fringe visibility. We therefore use white-light interferometry to get within a micron, and far-field measurements to optimize within 0.1 micron. Finer control should be possible with refined diagnostic techniques.

One can obtain near-field fringes of high visibility using amplitude division (whole aperture) beamsplitting such as occurs in a Mach-Zehnder (or Michelson) interferometer.[4] Such a beamsplitter provides two beams which are spatially mutually coherent for any beam, while partial-aperture beamsplitting, such as that used by us, places strict spatial coherence requirements on the master oscillator beam in order to obtain high visibility near-field fringes. We therefore use the near-field techniques to get close to zero OPD (within a wavelength). Near-field fringes are useful for this "coarse" search, because if tilt is introduced, the pattern displays many path length differences at a time. Our far-field measurements, discussed below, display the fact that the brightness of the focused spot is sensitive to twentieth-wavelength excursions in OPD (indeed it goes from a peak to a null within a half-wavelength), and therefore far-field diagnostics are required to optimize phased array performance.

The far-field focused spots of the individual, separated beams is shown in Fig. 9. They are nearly Gaussian in profile, and have the expected diffraction-limited width corresponding to their size in the near field. The beams were then overlapped in the far field, and the optical trombone was moved in very small (twentieth of a wavelength) steps until an intensity null was achieved in the center of the focused spot. This null, shown in Fig. 10a, is easier to observe than the optimum on-axis peak which appears in Fig. 10b. These two features occur with a half-wavelength excursion in OPD, which is a quarter-wavelength translation of the optical trombone. The narrowing of the focused spot in the direction of the rotating mirror scan is the expected result for coherent combination of the two beams for our near-field aperture and 90% mutual coherence. The peak brightness was occasionally near the expected result, but is such a sensitive function of OPD that only 2.5 times the single-beam brightness could be measured reproducibly.
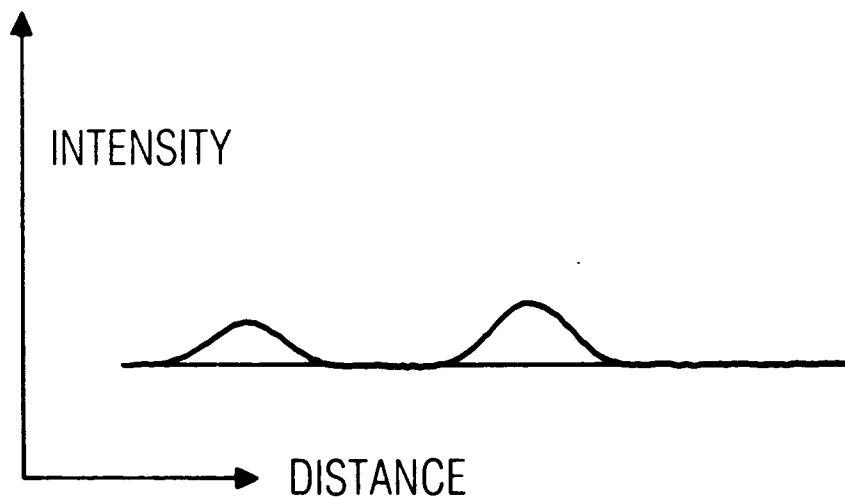

Fig. 9. Horizontal Scans of the Multiline Far-Field Spots with Amplification, When the Beams are Separated
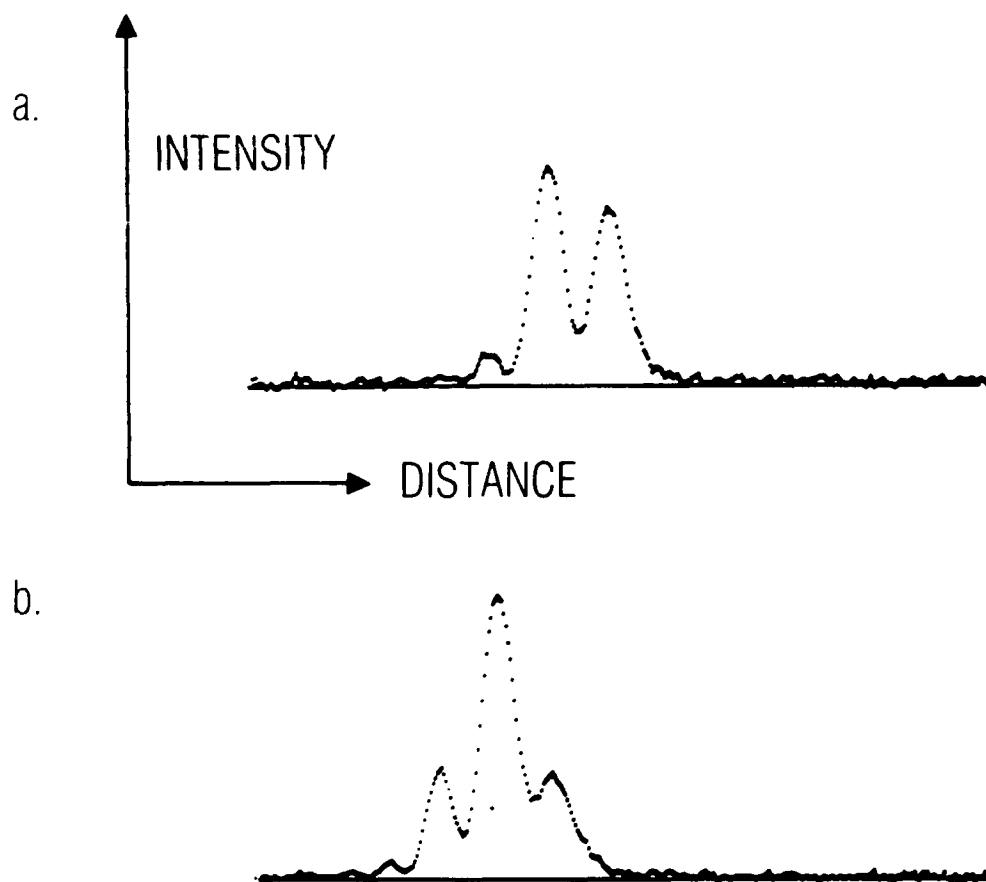
Fig. 10.   Horizontal Scan of the Multiline Far-Field Spot
with Amplification, When the Beams are Overlapped,
and (a) When the OPD is One-Half Wavelength from
Zero, and (b) When the OPD is Within a Twentieth-
Wavelength of Zero

VI. CONCLUSIONS

The Master Oscillator with Power Amplifiers configuration has been shown to be a viable technique for obtaining phased arrays of multiline CW HF chemical lasers. The nature of the HF amplifying medium is such that significant spectral mismatch is accommodated, and that the mutual coherence of the master oscillator beam is preserved. The engineering considerations for path length diagnostic and control were discussed, and the utility of first near-field, and then far-field, measurements was emphasized. The on-axis null a half-wavelength from zero OPD was shown to be helpful in finding zero OPD. Finally, the sensitivity of the focussed spot to twentieth-wavelength OPD is not surprising, as we specify the same tolerance on the surface figure of all of our mirrors. Our conclusion is that the process of amplification of HF laser beams does not affect their mutual coherence nor their beam quality, since we have measured nearly diffraction-limited output in the far field with or without it.

REFERENCES

1. W. R. Warren, *The Parallel Internal-Master-Oscillator Power Amplifier for Phase Matching the Output Beams of Multiline Lasers*, TR-0078(9990)-6, The Aerospace Corporation, El Segundo, CA 90245 (1978).

2. C. P. Wang, "Master and Slave Oscillator Array System for Very Large Multiline Lasers," *Appl. Opt.* 17, 83 (1978).

3. R. W. F. Gross, J. G. Coffer, R. A. Chodzko, and E. B. Turner, *Interference Patterns Produced by a Mach-Zehnder Interferometer and a Multiline HF Laser*, TR-0080(5764)-2, The Aerospace Corporation, El Segundo, CA 90245 (1980).

4. J. G. Coffer, J. M. Bernard, R. A. Chodzko, E. B. Turner, R. W. F. Gross, and W. R. Warren, "Experiment with Active Phase Matching of Parallel-Amplified Multiline HF Laser Beams by a Phase-Locked Mach-Zehnder Interferometer," *Appl. Opt.* 22, 142 (1983).

5. C. P. Wang, "Frequency Stability of a CW HF Chemical Laser," *J. Appl. Phys.* 47, 221 (1976).

6. D. J. Spencer, H. Mirels, and D. A. Durran, "Performance of CW HF Chemical Laser with N_2 or He Diluent," *J. Appl. Phys.* 43, 1151 (1972).

The Aerospace Corporation functions as an "architect-engineer" for national security projects, specializing in advanced military space systems. Providing research support, the corporation's Laboratory Operations conducts experimental and theoretical investigations that focus on the application of scientific and technical advances to such systems. Vital to the success of these investigations is the technical staff's wide-ranging expertise and its ability to stay current with new developments. This expertise is enhanced by a research program aimed at dealing with the many problems associated with rapidly evolving space systems. Contributing their capabilities to the research effort are these individual laboratories:

Aerophysics Laboratory: Launch vehicle and reentry fluid mechanics, heat transfer and flight dynamics; chemical and electric propulsion, propellant chemistry, chemical dynamics, environmental chemistry, trace detection; spacecraft structural mechanics, contamination, thermal and structural control; high temperature thermomechanics, gas kinetics and radiation; cw and pulsed chemical and excimer laser development including chemical kinetics, spectroscopy, optical resonators, beam control, atmospheric propagation, laser effects and countermeasures.

Chemistry and Physics Laboratory: Atmospheric chemical reactions, atmospheric optics, light scattering, state-specific chemical reactions and radiative signatures of missile plumes, sensor out-of-field-of-view rejection, applied laser spectroscopy, laser chemistry, laser optoelectronics, solar cell physics, battery electrochemistry, space vacuum and radiation effects on materials, lubrication and surface phenomena, thermionic emission, photo-sensitive materials and detectors, atomic frequency standards, and environmental chemistry.

Computer Science Laboratory: Program verification, program translation, performance-sensitive system design, distributed architectures for spaceborne computers, fault-tolerant computer systems, artificial intelligence, micro-electronics applications, communication protocols, and computer security.

Electronics Research Laboratory: Microelectronics, solid-state device physics, compound semiconductors, radiation hardening; electro-optics, quantum electronics, solid-state lasers, optical propagation and communications; microwave semiconductor devices, microwave/millimeter wave measurements, diagnostics and radiometry, microwave/millimeter wave thermionic devices; atomic time and frequency standards; antennas, rf systems, electromagnetic propagation phenomena, space communication systems.

Materials Sciences Laboratory: Development of new materials: metals, alloys, ceramics, polymers and their composites, and new forms of carbon; non-destructive evaluation, component failure analysis and reliability; fracture mechanics and stress corrosion; analysis and evaluation of materials at cryogenic and elevated temperatures as well as in space and enemy-induced environments.

Space Sciences Laboratory: Magnetospheric, auroral and cosmic ray physics, wave-particle interactions, magnetospheric plasma waves; atmospheric and ionospheric physics, density and composition of the upper atmosphere, remote sensing using atmospheric radiation; solar physics, infrared astronomy, infrared signature analysis; effects of solar activity, magnetic storms and nuclear explosions on the earth's atmosphere, ionosphere and magnetosphere; effects of electromagnetic and particulate radiations on space systems; space instrumentation.